# High-Temperature Reactions of Fullerene $C_{60}$ with H and OH

**T. Sommer and P. Roth***

*Institut für Verbrennung und Gasdynamik, Gerhard-Mercator-Universität Duisburg, D-47048 Duisburg, Germany*

*Received: October 10, 1997; In Final Form: January 21, 1998*

The reactions of H atoms and OH radicals with fullerene $C_{60}$ were studied behind reflected shock waves by time-dependent absorption measurements. Shock-heated mixtures of $C_2H_5I$ highly diluted in argon were used as a source for H atoms, and their absorption at $\lambda = 121.6$ nm was monitored using the highly sensitive ARAS technique. In a second series of experiments OH radicals were generated in $H_2/N_2O/Ar$ reaction systems, and the absorption of OH was monitored at $\nu = 32\,403.41$ cm$^{-1}$ using ring dye laser absorption spectroscopy (RDLAS). In each case, the respective mixtures were perturbed by $C_{60}$. Simultaneously with the absorption measurements, emission spectroscopy with an intensified CCD camera was used to acquire additional information about the reaction systems. The H atom experiments were performed at temperatures between 2100 and 2300 K, while OH absorption was measured in the temperature range 2020 K $\leq T \leq$ 2540 K. Postshock pressures were around 1.30 bar for all experiments. From the H-absorption measurements, an upper limit for the reaction $C_{60}$ + H to products (R9) ($k_9 < 1.0 \times 10^{12}$ cm$^3$ mol$^{-1}$ s$^{-1}$) was determined. For the $H_2/N_2O/Ar$ + $C_{60}$ reaction system, different kinetic models were discussed to verify the measured OH absorption. The reaction $C_{60}$ + OH to products (R7) ($k_7 = 1.0 \times 10^{15}$ exp(−6030 K/$T$) cm$^3$ mol$^{-1}$ s$^{-1}$) with the given rate coefficient represents the experimental findings quite well.

## Introduction

Since the discovery of fullerenes by Kroto et al. in 1985,[1] extensive investigations have been performed to study chemical and physical properties of this stable modification of elementary carbon. Fullerenes are discussed as having an influence on combustion processes and soot formation,[2,3] and its formation has been observed in benzene and acetylene−oxygen flames.[4] From the great variety of fullerenes, special attention is directed to the soccer-ball-shaped $C_{60}$ molecule, in which the carbon atoms are placed at the edges of 12 pentagons and 20 hexagons. In contrast to many investigations concerning the thermal stability of fullerene molecules, the chemical stability at high temperatures has not been studied in detail yet, although this may give insights into modern aspects of combustion chemistry and other scientific areas. Despite the great interest concerning the chemical stability of fullerenes, reliable kinetic data for fullerene reactions with atomic or radical species at high temperatures are still limited. The chemical stability of fullerenes with respect to molecular species such as NO, $SO_2$, $H_2$, CO, $NH_3$, and $O_2$ has been investigated by Zhang et al.[2] at room temperature. The conversion of $C_{60}$ to amorphous carbon was also studied in a $O_2$ atmosphere, and the oxidation products CO and $CO_2$ were observed at moderate temperatures.[5] The high-temperature oxidation of $C_{60}$ by $O_2$ was investigated in a previous shock tube study of our group both by following the emission of $C_2$ and the infrared diode laser absorption of CO and $CO_2$.[6] A rate coefficient for the oxidation of $C_{60}$ by O atoms has recently been determined by time-dependent ARAS/MRAS measurements of O and CO.[7] A shock-tube study on the thermal stability of $C_{60}$ was performed earlier[8] by time-dependent RDLAS measurements of $C_2$, which is the primary product during fullerene decomposition. From this study a temperature limit for the thermal stability of $C_{60}$ of $T \leq 2650$ K was determined as being relevant for shock-tube conditions.

The aim of the present work is to study the reactions of $C_{60}$ with H and OH by monitoring both concentrations in high-temperature experiments by spectroscopic absorption techniques. For this purpose, shock-heated mixtures of $C_2H_5I$ highly diluted in argon were used as a well-characterized source for H atoms. OH radicals were generated in high-temperature $H_2/N_2O/Ar$ mixtures. In each case the respective reaction systems were perturbed by addition of $C_{60}$. To ensure direct reactions of $C_{60}$ with the atomic or radical species, the mixtures were heated to temperatures below 2650 K. Three different diagnostic tools were used to follow the shock-induced processes. The sensitive ARAS technique was applied to monitor H atoms at $\lambda = 121.6$ nm, and RDLAS at $\nu = 32\,403.41$ cm$^{-1}$ was used to determine OH radical concentration. Simultaneously, emission spectroscopy with an intensified CCD camera was used to acquire further information about additional species such as $C_2$ or CH.

## Experimental Section

The experimental setup is described elsewhere,[7,8] and the main diagnostics used during the present study are schematically shown in Figure 1. They consist of an aerosol generator for dispersing the fullerene powder, the main shock tube for heating the fullerene containing mixtures to high temperatures, an ARAS spectrometer for measuring H atom absorption, a ring dye laser spectrometer for monitoring OH radicals, a spectrograph with intensified CCD camera for the detection of spectral and time-resolved emission, and an infrared diode laser system.

The $C_{60}$ powder was dispersed in argon by an expansion wave-driven aerosol generator.[9] It consists of a glass vessel of $V = 3 \times 10^4$ cm$^3$ volume connected to a glass tube of 5 cm inner diameter, which was separated by a thin diaphragm from the high-pressure tube. A thin dispersion plate was positioned

* To whom correspondence should be addressed.

S1089-5639(97)03304-5 CCC: $15.00 
Published on Web 04/11/1998

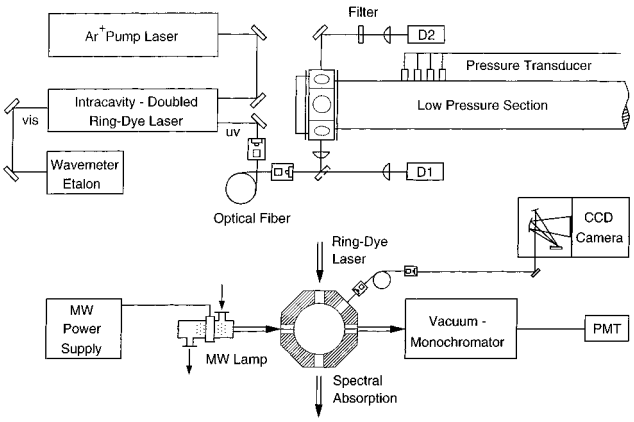


**Figure 1.** Schematic of the experimental setup including shock tube and different optical diagnostics.

near the diaphragm, which carried about 100 mg of the fullerene powder for each experiment. Before starting powder dispersion, the low-pressure section of the aerosol generator was evacuated to a pressure of about $5 \times 10^{-5}$ mbar. Subsequently, argon was filled into the high-pressure tube. After bursting of the diaphragm, the high-pressure argon gas expanded in the form of a supersonic expansion wave into the evacuated vessel, thus dispersing the fullerene powder and bringing it into aerosol form. The fullerene $C_{60}$ powder used during the present experiments was supplied by Hoechst AG, Germany, with a purity greater than 99.7%. The generated aerosol was mixed with either $C_2H_5I$/Ar or $H_2/N_2O$/Ar mixtures and subsequently filled into the running section of the main shock tube.

The stainless steel shock tube used as an isothermal−isobaric wave reactor has an inner diameter of 8 cm, a total length of 11 m, and a running section of 7.2 m in length. The initial pressure of the aerosol measured by calibrated diaphragm type pressure transducers was in the range from 19 to 30 mbar. The shock velocity was measured by four piezoelectric pressure transducers positioned at known distances along the shock tube axis. The postshock temperature and pressure were calculated from the incident shock speed by applying one-dimensional conservation equations. The shock wave running into the fullerene containing aerosol causes a sudden temperature and pressure increase, thus initiating the evaporation of the solid fullerene particles in less than 5 $\mu$s. Subsequently, the fullerene vapor started to react due to homogeneous gas-phase reactions[8,10] with the gas-phase radicals being formed in the described way.

The optical setup for measuring time-dependent H atom absorption consists of a microwave discharge lamp, the optical absorption path, a vacuum-UV monochromator, and a solar blind photomultiplier. The Lyman-$\alpha$ transition was excited in a gas mixture of He containing 1% of $H_2$ passing through the lamp at a pressure of 5 mbar. The $H_\alpha$ line was selected by a $^1/_5$ m vacuum-UV monochromator. To obtain the relation between measured absorption and the corresponding H atom concentration, the ARAS diagnostic was calibrated. For this purpose, gas mixtures of $H_2/N_2O$ highly diluted in argon with great excess of $H_2$ were shock-heated, and the absorption of H was measured and related to calculated species concentration based on kinetic data reported in the literature.[11,12] The calibration for H atoms, not shown here, can be well approximated by a modified Lambert−Beer law:

$$A(\mathrm{H}_\alpha) = 1 - \exp\left[-1.0 \times 10^{-11}\,\frac{L}{\mathrm{cm}}\left(\frac{[\mathrm{H}]}{\mathrm{cm}^{-3}}\right)^{0.8}\right] \qquad (1)$$

The ring dye laser spectrometer for measuring time-dependent OH absorption consists of a ring dye laser (Coherent 899-01 with Etalon assembly), which was intracavity frequency doubled using an angle-tuned $LiIO_3$ crystal. The laser was run with Sulforhodamine B (Kiton Red LC 6200) and pumped at 514.5 nm with an actively stabilized 6.5 W argon ion laser. In this way 10 mW of single-mode UV power was generated. The structure of the fundamental cavity mode was monitored by a scanning interferometer with 2 GHz free spectral range, and the wavelength of the visible output was measured by a Burleigh WA20 wavemeter. The UV laser beam was coupled into the measurement section of the shock tube by an optical fiber, and the time-dependent OH absorption during the high-temperature reactions was determined with a fast Si detector. A second Si detector was used to record the incident laser light intensity. The laser was fixed to the line center wavenumber at $\nu = 32\,403.41$ cm$^{-1}$ corresponding to the $Q_1(5)$ line of the $A^2\Sigma^+ \leftarrow X^2\Pi$ transition of OH. The calculated shape of the $Q_1(5)$ absorption line based on spectroscopic data reported in the literature[13−15] was experimentally confirmed in a series of additional shock-tube experiments in $H_2/N_2O$/Ar mixtures. The agreement between the calculated and measured line shape of the Doppler- and collision-broadened absorption line was excellent. The absorption profiles were stored in a transient recorder and then transmitted to a personal computer for further data processing.

The light emitted from the shock-heated reactive gas mixture was focused via a light fiber at the entrance slit of a $^1/_8$ m spectrograph with a spectral range of $\Delta\lambda = 255$ nm and a resolution of 1.3 nm. The spectrally resolved light was detected by an intensified CCD camera allowing a fast time shift of the optical information. For this purpose only a few lines at the top of the CCD sensor chip were illuminated for a certain time interval. The stored spectral emission was transferred stepwise line by line into the dark zone of the CCD chip, which served as a memory. In this way, the spectral and the temporal behavior of the emitted light was recorded. Spectral characteristics of the quantum efficiency of the intensifier and of the diffraction grid were taken into account. The intensified CCD camera system (Streak Star) with spectrograph was supplied by L.A.Vision.

For a quantitative data interpretation in terms of kinetic parameters, the initial concentration of $C_{60}$ was required. For this purpose fullerene $C_{60}$ powder was dispersed in Ar containing about 6% $O_2$. The aerosol mixtures were heated by the shock wave to conditions similar to the experiments of the present study, and this resulted in a complete oxidation of $C_{60}$ by $O_2$. The gas-phase oxidation products CO and $CO_2$ were quantitatively measured by tunable infrared diode laser spectroscopy, from which an initial $C_{60}$ gas-phase concentration of about 40 ppm could be deduced; see refs 8 and 10.

## Results

**H Atom Absorption in $C_2H_5I$/Ar + $C_{60}$ Systems.** The experiments in high-temperature $C_2H_5I$/Ar + $C_{60}$ mixtures were performed behind reflected shock waves in the temperature range 2100 K $\leq T \leq$ 2300 K at pressures around 1.3 bar. In a series of experiments with $C_2H_5I$ concentrations ranging between 0.5 and 2 ppm, the absorption by H atoms was monitored with and without addition of $C_{60}$. Some additional experiments were performed to quantify the absorption at $\lambda = 121.6$ nm in pure mixtures of $C_{60}$/Ar without any addition of $C_2H_5I$. The measured absorption was always very low. Simultaneously with all ARAS absorption measurements, the spectral and time-resolved emission of the reacting mixtures was recorded.

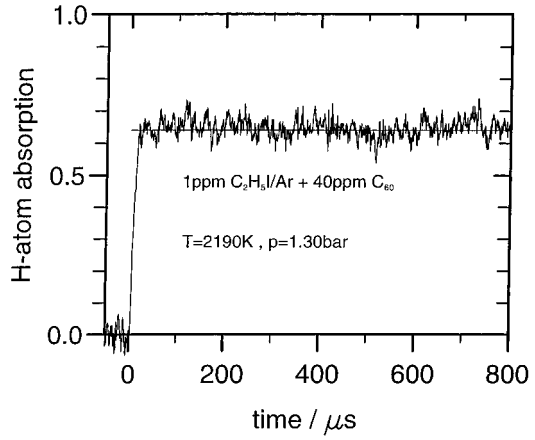


**Figure 2.** Typical H atom absorption signal measured in a 1 ppm $C_2H_5I$/Ar mixture with addition of 40 ppm $C_{60}$.

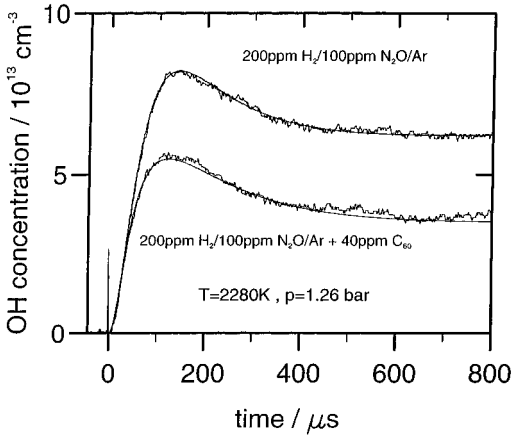


**Figure 3.** Two examples of time-dependent OH concentrations measured under similar conditions in $H_2/N_2O$/Ar mixtures with and without addition of $C_{60}$ (noisy lines). The solid lines correspond to kinetic simulations (see text).

A typical example of H atom absorption obtained from a shock-heated $C_2H_5I$/Ar mixture with addition of 40 ppm $C_{60}$ is shown in Figure 2. The absorption profile shows a fast increase after shock arrival followed by a steady-state behavior for the remaining observation time. With respect to the H atom calibration of eq 1, the measured absorption of approximately 65% corresponds very well with the initial $C_2H_5I$ concentration of 1 ppm. The absorption signal measured under similar conditions without $C_{60}$ was identical within the uncertainty of the ARAS diagnostic. This principal behavior was observed in all experiments with and without addition of $C_{60}$; i.e., no consumption of H atoms caused by $C_{60}$ was observed for the conditions of the present experiments. The experiments in $C_{60}$/Ar mixtures without addition of $C_2H_5I$ showed no spectral absorption at $\lambda = 121.6$ nm. The spectral- and time-dependent resolved emission measurements using the CCD camera system showed no characteristic radiation for all experiments. Especially $C_2$ and CH, which have strong spectroscopic bands within this region, could not be observed during the present study.

**OH Absorption in $H_2/N_2O$/Ar + $C_{60}$ Systems.** The experiments in high-temperature $H_2/N_2O$/Ar + $C_{60}$ mixtures were also performed behind reflected shock waves in the temperature range 2020 K $\leq T \leq$ 2540 K at pressures around 1.3 bar. The initial reactant concentrations were 200 ppm $H_2$ and 100 ppm $N_2O$. The absorption by OH radicals was monitored by narrow-bandwidth RDLAS at $\nu = 32\,403.41$ $cm^{-1}$.

Typical examples of measured absorption profiles converted to absolute OH concentration from shock-heated $H_2/N_2O$/Ar mixtures with and without perturbation by $C_{60}$ are illustrated in Figure 3, see noisy lines. The OH profile obtained in the experiment without $C_{60}$ shows a fast increase after shock arrival and a characteristic decrease after reaching maximum concentration, followed by a steady-state behavior for the rest of the observation time. The measured OH concentration with addition of $C_{60}$ is significantly lower by a factor of approximately 1.7, but the time evolution of the profile is very similar to that of the unperturbed experiment. This principal behavior was found in all experiments. Compared to the results in pure $H_2/N_2O$/Ar mixtures, the addition of $C_{60}$ reduced the OH concentration by factors between 1.6 and 2.1, depending on the respective temperature. Again, the emission measurements did not show any characteristic spectral radiation.

## Discussion

It can be assumed that several subsequent processes occur in shock-heated gases containing $C_{60}$ in highly dispersed particle form. Due to the relatively high vapor pressure of $C_{60}$, the solid agglomerated carbonaceous particles evaporate rapidly at high temperatures. This process starts behind the incident shock wave, where temperatures are in the range 1000 K $\leq T \leq$ 1300 K, and continues behind the reflected wave much more rapidly because of the higher temperature level. The particle size after powder dispersion was determined by scanning electron microscopy, resulting in mean particle diameters of less than 900 nm. An upper limit for a fullerene particle evaporation time of about 5 $\mu$s can be calculated for conditions of the present study.[16] The given upper limit for the evaporation time was experimentally confirmed by laser light scattering experiments behind shock waves.[10] We therefore can assume for our experimental conditions that the initial reactant $C_{60}$ is in the vapor phase for nearly the complete observation time and that reactions described in this study are dominated by homogeneous gas-phase kinetics.

**H Atom Absorption in $C_2H_5I$/Ar + $C_{60}$ Systems.** The dissociation of $C_2H_5I$ at high temperatures is well-known and has frequently been used as a pyrolytic source for H atoms.[17] In gas mixtures of relatively low initial reactant concentration and at temperatures above 1200 K, the decomposition of $C_2H_5I$ is followed by the fast decay of the ethyl radical, thus forming H atoms.

$$C_2H_5I \rightarrow C_2H_5 + I$$

$$C_2H_5 \rightarrow C_2H_4 + H$$

All H atom absorption profiles measured in $C_2H_5I$/Ar mixtures with and without $C_{60}$ show a very fast increase after arrival of the reflected shock wave, followed by a steady-state behavior for the rest of the observation time. The concentration of H atoms calculated from the respective absorption via eq 1 was in excellent agreement with the initial $C_2H_5I$ concentration, and no absorption at $\lambda = 121.6$ nm was observed in experiments with pure $C_{60}$/Ar mixtures. We therefore can assume that all H-atoms measured in $C_{60}/C_2H_5I$/Ar systems were formed by thermal decomposition of $C_2H_5I$. A decrease of H atoms caused by the addition of $C_{60}$ could not be observed in any experiment of the present study. Mixtures of higher initial $C_{60}$ gas-phase concentration, which would increase the consuming rate of H atoms, could not be used due to the specific aerosol generation process. Furthermore, experiments at higher temperatures could not be performed with respect to the thermal decomposition of

$C_2H_4$ and $C_{60}$. For that reason, the experimental results obtained in $C_2H_5I/Ar + C_{60}$ mixtures are sufficiently suitable to estimate an upper limit for rate coefficient $k_9$ for the consumption of H atoms by $C_{60}$. If we consider the direct reaction

$$C_{60} + H \rightarrow \text{products} \qquad \text{(R9)}$$

to be responsible for a decrease in the H concentration without any significant secondary reactions, we can calculate the time evolution for H atoms, [H]($t$), by simple first-order kinetics, taking the great excess of $C_{60}$ into account:

$$[H](t) = [H]_0 \exp(-k_9[C_{60}]_0 t)$$

$[H]_0$ and $[C_{60}]_0$ denote the respective initial gas-phase concentrations after shock arrival. If we further assume that a decrease in H atom concentration of 20% within the observation time of 800 $\mu$s would be measurable with the ARAS diagnostic, we can estimate an upper limit for $k_9$ being relevant for typical conditions of the present study ($T = 2200$ K, $p = 1.3$ bar) by

$$k_9 \leq \frac{-\ln(0.8)}{[C_{60}]_0 \times 800\ \mu s} \approx 1.0 \times 10^{12}\ \text{cm}^3\ \text{mol}^{-1}\ \text{s}^{-1}$$

For comparison, the reaction of O atoms with $C_{60}$, which has recently been investigated in our group,[7] is much faster. A rate coefficient was determined in the temperature range 1870 K $\leq T \leq$ 2625 K by O atom ARAS measurements in $N_2O/Ar + C_{60}$ mixtures and was found to be

$$k_8 = 3.0 \times 10^{15} \exp(-11450\ \text{K}/T)\ \text{cm}^3\ \text{mol}^{-1}\ \text{s}^{-1}$$

For temperatures around $T = 2200$ K, rate coefficient $k_8$ is more than 1 order of magnitude higher compared to the evaluated upper limit for $k_9$.

**OH Absorption in $H_2/N_2O/Ar + C_{60}$ Systems.** In the past, numerous experimental[11,18] and theoretical[19,20] studies have been performed to determine and verify hydrogen−oxygen kinetics. In the present work, OH time histories measured in pure $H_2/N_2O$/Ar mixtures were well reproduced by simulations with the CHEMKIN program package[21] using the mechanism and rate coefficients reported by Masten et al.[11] To simplify this mechanism of 23 elementary reactions with respect to our experimental conditions, a detailed sensitivity analysis was performed to study the contribution of each reaction to the computed OH concentration. With the normalized sensitivity coefficients defined by

$$S_{X,i} = \frac{k_i}{[X]} \frac{\partial [X]}{\partial k_i}$$

the influence of variations in the rate coefficients was analyzed. In this way, reactions of minor importance were eliminated, and a reduced mechanism of six reactions given in the upper part of Table 1 was derived being relevant for the description of the present OH source. Rate coefficients for the kinetic simulations given by Masten et al.[11] are also summarized in Table 1. An individual example comparing a measured and a calculated OH profile based on the reduced mechanism (R1) to (R6) of Table 1 is illustrated in Figure 3; see upper traces for the experiment without $C_{60}$. Nearly complete agreement between experiment and simulation was obtained for this as well as for all other experiments. The mechanism therefore seems to be sufficient to characterize the time-dependent OH source.

**TABLE 1: Simplified High-Temperature Reaction Mechanism of the $H_2/N_2O + C_{60}$ System Highly Diluted in Ar[a]**

| no. | reaction | $A$ | $n$ | $B$ | ref |
|---|---|---|---|---|---|
| (R1) | $N_2O + M \rightleftharpoons N_2 + O$ | $9.28 \times 10^{14}$ | 0.0 | 29920 | 11 |
| (R2) | $N_2O + H$ h $N_2 + OH$ | $7.60 \times 10^{13}$ | 0.0 | 7604 | 11 |
| (R3) | $OH + H_2 \rightleftharpoons H_2O + H$ | $1.17 \times 10^{9}$ | 1.30 | 1826 | 11 |
| (R4) | $H + O_2 \rightleftharpoons OH + O$ | $9.33 \times 10^{13}$ | 0.0 | 7453 | 11 |
| (R5) | $O + H_2 \rightleftharpoons OH + H$ | $5.06 \times 10^{4}$ | 2.67 | 3168 | 11 |
| (R6) | $OH + OH \rightleftharpoons H_2O + O$ | $6.00 \times 10^{8}$ | 1.30 | 0 | 11 |
| (R7) | $C_{60} + OH \rightarrow$ products | $1.00 \times 10^{15}$ | 0.0 | 6030 | this study |
| (R8) | $C_{60} + O \rightarrow$ products | $3.00 \times 10^{15}$ | 0.0 | 11450 | 7 |
| (R9) | $C_{60} + H \rightarrow$ products | $\leq 1.00 \times 10^{12}$ | 0.0 | 0 | this study |

[a] $k_i = A \times T^n \exp(-B/T)$. Backward rate coefficients calculated based on CHEMKIN thermodynamic data.

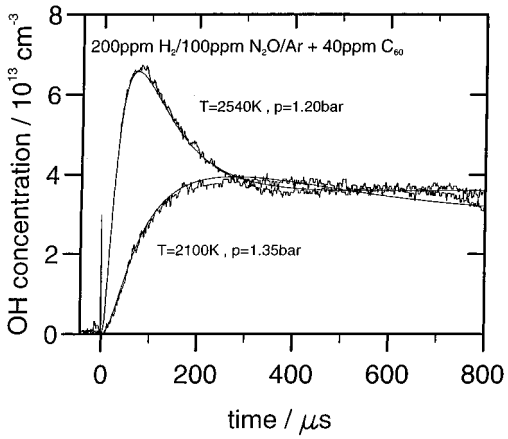


**Figure 4.** Comparison between measured (noisy lines) and calculated (solid lines) OH concentration profiles for two different temperatures.

In contrast to the $C_2H_5I/Ar$ reaction system, in which free radicals are generated directly by dissociation of the initial reactant, the formation of H, O, and OH in $H_2/N_2O/Ar$ mixtures is controlled by chain-propagating and chain-branching reactions.[11] The steady-state concentrations of the chain carrier OH measured at later reaction times result from the quasi-equilibration of reactions R1 to R6. A consumption of OH by reaction with $C_{60}$ will partly be compensated by a further formation of OH by the chain mechanism, depending on the concentration of O and H atoms. Therefore, perturbation of the reaction system by $C_{60}$ does not result in a continuous decrease of OH. Thus, it seems reasonable to interpret the observed strong change in OH caused by the addition of $C_{60}$ (see Figure 3) by direct reactions of fullerenes with OH, O, and H; see lower part of Table 1. Reactions of the species $H_2$, $O_2$, $N_2$, $N_2O$, and $H_2O$ with $C_{60}$, which are also present in the reaction system, were not considered due to their relatively low reactivity. The influence of possible secondary reactions will be discussed later in more detail.

As a first step of data interpretation, we assumed the three fullerene reactions and studied their influence on the measured OH profiles. For each individual shock-tube experiment, the measured absorption was converted to absolute species concentration and compared to computer profiles based on the mechanism of Table 1. The rate coefficient $k_7$ was a variable parameter to achieve a good fitting, while $k_8$ was taken from the earlier performed O atom ARAS experiments. The upper limit derived from the H atom ARAS measurements of the present study was used for $k_9$. Examples of best fits for different shock tube experiments are illustrated in Figure 3 (see lower trace) and Figure 4. Nearly complete agreement between calculated and measured concentrations for the examples as well

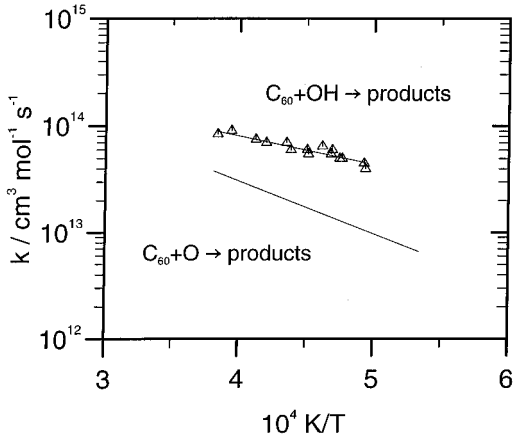


**Figure 5.** Arrhenius diagram for rate coefficient $k_7$, determined in the present study, and $k_8$, reported earlier.

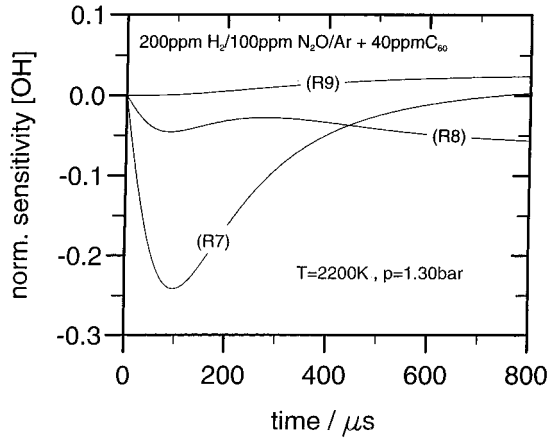


**Figure 6.** Normalized sensitivity coefficients (see text) of reactions R7−R9 describing the influence on OH concentration.

as for all other experiments was obtained. It seems that the rather simple mechanism is sufficient to describe the OH perturbation experiments in terms of a rate coefficient $k_7$. Furthermore, the results indicate that reactions of expected fullerene fragments and other intermediate species, which were neglected in our data analysis, can only have a minor influence on the measured property. All individual rate coefficients $k_7$ obtained in this way are shown in the Arrhenius diagram of Figure 5. A least-squares fit to the data points represented by the solid line can be expressed by

$$k_7 = 1.0 \times 10^{15} \exp(-6030\ \mathrm{K}/T)\ \mathrm{cm^3\ mol^{-1}\ s^{-1}}$$

The scattering around the given mean value is comparatively low. For comparison, the Arrhenius expression for rate coefficient $k_8$ is also illustrated in Figure 5.

To get a better insight into the influence of the three fullerene reactions R7 to R9 on the computed OH profiles, a detailed sensitivity analysis of the mechanism was performed. Figure 6 shows examples of normalized sensitivity coefficients calculated as a function of time. The reaction conditions chosen were typical for the present perturbation experiments. At early reaction times, when OH profiles reach maximum concentration, the strongest influence is clearly correlated to (R7), while (R8) is less sensitive. Contrariwise, at later reaction times the influence of (R7) diminishes and the sensitivity of (R8) increases slowly. Reaction R9 does not significantly contribute to the calculated OH concentration. The sensitivity analysis illustrates that reaction R7 is dominant at early reaction times.

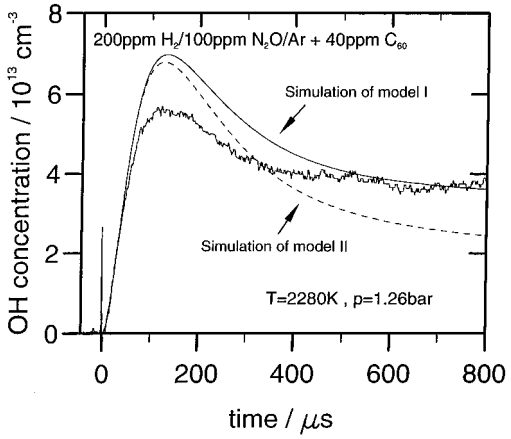


**Figure 7.** Kinetic simulations with $k_7 = 0$ illustrating the influence of single O atom (model I) and successive O atom reactions (model II) with $C_{60}$ and related fragments compared to measured OH time profile.

Additional computer simulations based on different models were performed to prove whether only O atom reaction with $C_{60}$ or its decomposition products, without any direct OH reaction, are suitable to explain the measured OH behavior. Typical examples compared to a measured profile are illustrated in Figure 7. The simulation of the upper trace (solid line) is based on the mechanism of Table 1 with $k_7 = 0$ (model I). For the lower trace (dotted line) $k_7$ was also set equal to zero, but subsequent reactions of O atoms and expected fullerene fragments were additionally considered (model II). For the computer simulations, model II was formally implemented to the mechanism of Table 1 in the following way:

$$C_{60} + O \rightarrow C_{59} + \text{products}$$

$$C_{60-x} + O \rightarrow C_{60-x-1} + \text{products};\quad x = 1, 2, \ldots \quad \text{(R8)}$$

It is obvious that the steady-state concentration at later reaction times is well approximated by model I, while the subsequent reactions of model II lead to a further decrease. For both kinetic models, the calculated maximum concentrations are very similar but do not agree with the measurements. For the simulation of model II, all rate coefficients were assumed to be equal to $k_8$, although fragments are expected to have a higher reactivity than $C_{60}$. In case of assuming more realistic higher rate coefficients for the reactions of fragments, the deviation between measured and calculated profiles at the end of the observation time would be even greater.

The remaining question of what species are the products of (R7) cannot be answered satisfactorily from the present experiments. In the earlier performed O atom perturbation study, CO has been identified as the main but probably not the only product of (R8). The addition reaction of O to the $\pi$ double bonds in $C_{60}$ has also been discussed as a second channel for fullerene oxidation.[7,22,23] In a similar way, the reaction of $C_{60}$ with OH may proceed via formation of HCO or by addition of OH to the fullerene cage, but in both cases the respective products could not be measured with our diagnostics. Furthermore, if we assume HCO being a product of (R7), the formation of additional H-atoms from the fast decomposition of HCO[12] would not significantly influence OH time histories with respect to the chain mechanism of Table 1. Therefore, a specific interpretation of (R7) with respect to a prediction of further reaction products is not possible from the present study.

## Conclusion

The reaction of fullerene $C_{60}$ with H atoms and with OH radicals has been studied in two different series of experiments by ARAS and RDLAS absorption measurements. Mixtures of $C_2H_5I$ or $H_2/N_2O$, in each case highly diluted in argon, were shock-heated and used as well-characterized thermal sources for H or OH. The reaction systems were perturbed by addition of $C_{60}$. In $C_2H_5I$/Ar systems, ARAS measurements of H atom concentration showed no significant reactivity of H atoms with $C_{60}$. An upper limit for a rate coefficient of a direct reaction $C_{60} + H \rightarrow$ products was evaluated. In the case of $H_2/N_2O$/Ar mixtures, the perturbation by $C_{60}$ caused a strong change of OH time histories. Different kinetic models were developed and compared with the experimental results. The measured OH concentration profiles were interpreted in terms of a rate coefficient for the reaction $C_{60} + OH \rightarrow$ products.

**Acknowledgment.** The authors thank N. Schlösser for her help in conducting the experiments. This work is originated in the Sonderforschungsbereich 209 of the Universität Duisburg. The financial support of the Deutsche Forschungsgemeinschaft is gratefully acknowledged.

## References and Notes

(1) Kroto, H. W.; Heath, J. R.; O'Brien, S. C.; Curl, R. F.; Smalley, R. E. $C_{60}$: Buckminsterfullerene. *Nature* **1985**, *318*, 162−163.

(2) Zhang, Q. L.; O'Brien, S. C.; Heath, J. R.; Liu, Y.; Curl, R. F.; Kroto, H. W.; Smalley, R. E. Reactivity of Large Carbon Clusters: Spheroidal Carbon Shells and Their Possible Relevance to the Formation and Morphology of Soot. *J. Phys. Chem* **1986**, *90*, 525−528.

(3) Lifshitz, C. Energetics and dynamics of ionization and dissociation of fullerene carbon clusters. *Mass Spectrom. Rev.* **1993**, *12*, 261−284.

(4) Gerhardt, P.; Löffler, S.; Homann, K. H. Polyhedral carbon ions in hydrocarbon flames. *Chem. Phys. Lett.* **1987**, *137*, 306−310.

(5) Chen, H. S.; Kortan, A. R.; Haddon, R. C.; Kaplan, M. L.; Chen, C. H.; Musjce, A. M.; Chou, H.; Fleming, D. A. Reactivity of $C_{60}$ in pure oxygen. *Appl. Phys. Lett.* **1991**, *59*, 2956−2958.

(6) von Gersum, S.; Roth, P. High-Temperature Pyrolysis and Oxidation of Fullerene $C_{60}$ Behind Shock Waves. *25th Symposium (International) on Combustion*; The Combustion Institute: Pittsburgh, PA, 1994; pp 661−669.

(7) Sommer, T.; Roth, P. High-Temperature Oxidation of Fullerene $C_{60}$ by Oxygen Atoms. *J. Phys. Chem. A* **1997**, *101*, 6238−6242.

(8) Sommer, T.; Kruse, T.; Roth, P. $C_2$ formation during high-temperature pyrolysis of fullerene $C_{60}$ in shock waves. *J. Phys. Chem.* **1995**, *99*, 13509−13512.

(9) Rajathurai, A. M.; Roth, P.; Fissan, H. A Shock and Expansion Wave-driven Powder Disperser. *Aerosol Sci. Technol.* **1990**, *12*, 613−619.

(10) von Gersum, S.; Kruse, T.; Roth, P. Spectral Emission During High-Temperature Pyrolysis of Fullerene $C_{60}$ in Shock Waves. *Ber. Bunsen-Ges. Phys. Chem.* **1994**, *98*, 979−982.

(11) Masten, D. A.; Hanson, R. K.; Bowman, C. T. Shock Tube Study of the Reaction $H + O_2 \rightarrow OH + O$ Using OH Laser Absorption. *J. Phys. Chem.* **1990**, *94*, 7119−7128.

(12) Warnatz, J. *Rate Coefficients in the C/H/O System*; Springer-Verlag: New York, 1984.

(13) Rea, E. C.; Chang, A. Y.; Hanson, R. K. Shock-tube Study of Pressure Broadening of the $A^2\Sigma^+$-$X^2\Pi$ (0,0) Band of OH by Ar and $N_2$. *J. Quant. Spectrosc. Radiat. Transfer* **1987**, *37*, 117−127.

(14) Smith, G. P.; Crosley, D. R. Quantitative Laser-Induced Fluorescene in OH: Transition Probabilities and the Influence of Energy Transfer. *18th Symposium (International) on Combustion*; The Combustion Institute: Pittsburgh, PA, 1980; p 1511.

(15) Goldman, A.; Gillis, J. R. Spectral Line Parameters for the $A^2\Sigma^-$-$X^2\Pi$ (0,0) Band of OH for Atmospheric and High Temperatures. *J. Quant. Spectrosc. Radiat. Transfer* **1981**, *25*, 111- -135.

(16) Fuller, E. N.; Schettler, P. D.; Giddings, J. C. A new method for predicting of binary gas-phase diffusion coefficients. *Ind. Eng. Chem.* **1966**, *58*, 19−27.

(17) Herzler, J.; Frank, P. High-Temperature Reactions of Phenylacetylene. *Ber. Bunsen-Ges. Phys. Chem.* **1992**, *96*, 1333−1338.

(18) Pirraglia, A. N.; Michael, J. V.; Sutherland, J. W.; Klemm, R. B. A Flash Photolysis-Shock Tube Kinetic Study of the H atom Reaction with $O_2$: $H + O_2 \rightleftharpoons OH + O$ (962 K ≤ $T$ ≤ 1705 K) and $H + O_2 + Ar \rightarrow HO_2 + Ar$ (746 K ≤ $T$ ≤ 987 K). *J. Phys. Chem.* **1989**, *93*, 282.

(19) Miller, J. A. Nonstatistical effects and detailed balance in quasi-classical trajectory calculations of the thermal rate coefficient for $O + OH \rightarrow O_2 + H$. *J. Chem. Phys.* **1986**, *84*, 6170−6177.

(20) Troe, J. Relation between Potential and Rate Parameters for Reactions on Attractive Potential Energy Surfaces. Application to the Reaction $HO + O \rightleftharpoons HO_2^* \rightarrow H + O_2$. *J. Phys. Chem.* **1986**, *90*, 3485.

(21) Kee, R. J.; Miller, J. A.; Jefferson, T. H. A general-purpose, problem-independent, transportable, fortran chemical kinetics code package. Sandia Report SAND80-8003, Sandia National Laboratories, Albuquerque, NM 87185, 1980.

(22) Wood, J. M.; Kahr, B.; Hoke, S. H.; Dejarme, L.; Cooks, R. G.; Ben-Amotz, D. Oxygen and Methylene Adducts of $C_{60}$ and $C_{70}$. *J. Am. Chem. Soc.* **1991**, *113*, 5907.

(23) Creegan, K. M.; Robbins, J. L.; Robbins, W. K.; Millar, J. M.; Sherwood, R. D.; Tindall, P. J.; Cox, D. M. Synthesis and Characterization of $C_{60}O$, the First Fullerene Epoxide. *J. Am. Chem. Soc.* **1992**, *114*, 1103−1105.